Behaviour and Design of Crest-fixed Profiled Steel Roof Claddings under Wind Uplift

M. Mahendran

School of Civil Engineering

Queensland University of Technology, Brisbane

Abstract

Profiled steel roof claddings in Australia are commonly made of very thin high tensile steel and are crest-fixed with screw fasteners. At present the design of these claddings is entirely based on testing. In order to improve the understanding of the behaviour of these claddings under wind uplift, and thus the design methods, a detailed investigation consisting of a finite element analysis and laboratory experiments was carried out on two-span roofing assemblies of three common roofing profiles. It was found that the failure of the roof cladding system was due to a local failure (dimpling of crests / pull-through) at the fasteners. This paper presents the details of the investigation, the results and then proposes a design method based on the strength of the screwed connections, for which testing of small scale roofing models and/or using a simple design formula is recommended.

Keywords

Crest-fixed profiled steel roof claddings, Finite element analysis, Laboratory experiments, Small scale models, Wind uplift, Screwed connections

1. Introduction

In Australia, profiled steel roof claddings are commonly made of very thin high tensile steel (G550 steel with a minimum yield strength of 550 MPa), have a maximum depth between 16 and 30 mm, and are crest-fixed with screw fasteners. In general, the common roof claddings fall into two main groups based on their fatigue behaviour under cyclic wind loading[1], and the geometry of the profile. They are shown in Figure 1. The corrugated roofing (arc and tangent type) represents the first group whereas the trapezoidal roofing which has trapezoidal ribs represents the second group.

During high wind events such as storms and cyclones, these claddings are subjected to uplift loading, and their static and fatigue behaviour have been found to be very complicated[1]. They are also susceptible to fatigue cracking during storms and cyclones, mainly because of crest-fixing[1,2]. Therefore at present their design is entirely based on laboratory testing of large scale roof claddings including both static and fatigue wind uplift tests[3,4,5]. European[6] and American[7] recommendations for profiled steel roof claddings cannot be used as they are for thicker, deeper and softer steel claddings fastened at the valleys, which are mainly subjected to gravity loading rather than uplift. Although testing produces reliable assessment of the strength of crest-fixed claddings, it is often time consuming and expensive, and thus inhibits innovation and advances in the steel roof sheeting industry. This is reflected by the limited number of roofing profiles in Australia in contrast to the vast number of more efficient profiles in Europe.

In order to improve the understanding of the behaviour of the crest-fixed profiled steel roof claddings used in Australia, and thus the design methods, a detailed investigation consisting of laboratory experiments and finite element analyses of roof claddings was carried out. In this investigation only the steel claddings which are crest-fixed using screw fasteners and normal washers (not cyclone washers) were considered. It is expected that when these claddings are fastened with the larger cyclone washer assemblies used in some

cyclone prone areas of Australia, their behaviour will be different. Two-span roofing assemblies of the three **common** roofing profiles with a base metal thickness of 0.42 mm (G550 steel) shown in Figures 1 a(i), b(i) and b(ii) were analysed and tested. The corrugated roofing in Figure 1 a(ii) was not included as its behaviour was expected to be similar to that of the other corrugated roofing profile. This paper presents the details of this investigation, the results and recommendations.

2. Experimental Investigation

A two-span roofing assembly with simply supported ends was considered adequate to model the critical regions of a multi-span roofing assembly under a uniform wind uplift pressure[1,8]. Three different test spans of 600, 900 and 1150 mm were chosen in order to represent the common prototype end spans. Roofing specimens of either one or two sheet width were fastened to timber battens at every crest for the trapezoidal roofing with wide pans (Type A), and at alternate crests for others (see Figure 1) by No.14 x 50/65 mm Type 17 self-drilling screws with EPDM seals[9]. The No.14 screws have head and shaft diameters of 14.5 and 5.1 mm, respectively, and the 2 mm thick rubber seals have outside and inside diameters of 11 and 5.5 mm. In a few earlier experiments air bags were used to simulate a uniform wind uplift pressure loading on roofing, however, because of the approximations that have to be made regarding the area of loading, layers of bricks were used as the loading medium for the later experiments. In the latter case the roofing assembly was set-up upside down, the troughs were first filled with sand, and then loaded with layers of bricks. In this manner, a uniform uplift loading which can be calculated without any approximations was applied to the roof cladding. Figure 2 shows the test set-up using brick loading.

During the experiments, deflections of roofing were measured at three important locations, namely at one of the screwed and unscrewed crests/pans at midspan and at one of the

unscrewed crests/pans at the central support. The central support reaction was measured using two load cells located at the ends of the support (see Figure 2), which enabled the determination of the average load per fastener at the critical central support. A simple formula was also used to calculate the same, given the magnitude of brick loading/air bag pressure. Experiments were continued until the roofing failed locally around the central support fasteners by either pull-through or dimpling of crests.

3. Finite Element Analysis

The same two-span roofing assemblies were analysed using a finite element program MSC/NASTRAN[10] to study their behaviour under a uniform wind uplift pressure loading. Isoparametric shell elements were used to model the roof cladding. The shell element was either a four-noded quadrilateral CQUAD4 (mainly) or a three-noded triangular element CTRIA3 with six degrees of freedom at each node. Both nonlinear geometric and material effects were included in the analysis. Details of the finite element program can be found elsewhere[10].

Because of the symmetry of the cladding and the loading and support conditions, roofing of one span long (600 and 900 mm) and an appropriate width equal to the pitch or half the pitch of the roofing profile (76 mm for corrugated roofing, 95 and 87 mm for Trapezoidal roofing Type A and B) was considered in the finite element analysis (FEA). Appropriate boundary conditions were used to model the discrete supports provided by the screw fastener heads. MSC/XL[10] was used to draw the cladding with relevant boundary conditions and to apply the loading and other conditions. Figure 3 shows the details of the finite element meshes of the three roof claddings. As seen in Figure 3, a finer mesh was used around the critical central support fastener hole in order to model adequately the local stresses and deformations in that area. The adequacy of the finite element meshes was verified using convergence studies. The analysis was carried out on a super computer

(Convex machine). Thus it was possible to use a reasonably fine mesh involving approximately 1200 nodes and 800 elements, and the results were obtained within 4 hours.

The material was modelled as perfect elastic-plastic and the material properties for the steel assumed were, Young's modulus = 200,000 MPa, Poisson's ratio = 0.3 and yield (0.2% proof) stress = 690 MPa. This yield stress was determined from tensile tests on specimens cut in the longitudinal direction from coil steel used to roll the roof claddings. The corresponding ultimate stress was 720 MPa. The high tensile steel exhibited very little strain hardening and had a failure strain of only 2%. The yield stress in the transverse direction was 770 MPa, but this difference in yield stress was ignored. No test was conducted to study the variation of material properties in the cross-section of profiled roof sheeting. However, past investigations[8] have indicated that there was little change in the material properties for corrugated roofing. It is believed that the sharp corners of trapezoidal roofing will have an increased yield stress, but this was not considered in the finite element analysis. Effects due to the presence of initial geometric imperfections in the roof cladding and the residual stresses due to cold-forming were also not considered in the finite element modelling. It was considered that the overall effects of the above approximations on the results would be negligible.

4. Results and Discussions

For each roofing profile considered in this investigation, the load-deflection curves obtained from the FEA and experiments are presented first, and the behaviour of roofing is discussed based on the results. The load-deflection curves are presented in the format of load per fastener and wind uplift pressure versus upward deflections at three important locations. The experimental tensile load per fastener was calculated from the measured uniform pressure using a simple formula as shown next.

$$\text{Load per fastener} = \alpha \times \text{Wind pressure} \times \text{Span} \times \text{Distance between fasteners} \qquad (1)$$

where the coefficient $\alpha = 1.25$

The load per fastener value from Equation (1) was generally greater than the average load per fastener measured directly from the central support load cells. It appeared that the coefficient 1.25 in the simple formula, which is based on linear theory assuming elastic material and no cross-section distortion, had to be revised depending on the roofing profile and level of loading to a lower value in the range from 1.15 to 1.25 in order to obtain the actual load per fastener. The FEA load per fastener was obtained from the reaction output, which also confirmed the above observations. Therefore in all the load-deflection curves, the load per fastener obtained directly from the central support load cell measurements in experiments and from the reaction force output in the FEA were used.

4.1 Corrugated Roofing Profile

The load-deflection curves for the roofing of 900 mm span from both experiments and FEA are presented in Figure 4, and they appear to be in good agreement.

As seen in Figures 4 and 5, the uplift loading caused severe cross-sectional distortion of the discretely fastened roofing (at alternate crests only). During experiments this led to a localised plastic deformation (dimpling) of crests (Figure 6) at a load of 870 N per fastener (N/f). The corresponding uplift pressure was 5.27 kPa. There was no buckling or global yielding of the section at this point. The FEA predicted 815 N/f and 5.18 kPa, indicating good agreement between the two results. The regions around the fastener holes were yielding at this stage. Despite the local failure at the crests, the roofing had reserve static strength beyond this load. The FEA showed that only the region around the central support fastener hole was yielding, and this yielding was largely due to localised bending deformations (see Figure 6).

In this investigation loading was discontinued soon after dimpling of crests had occurred as it was considered to be the limiting case. The reserve static strength beyond the dimpling

of crests is of no importance, particularly from a fatigue point of view[1]. Further details of the behaviour of corrugated roofing, in particular, beyond the local dimpling failure can be found elsewhere[8].

Experiments and FEA of a 600 mm span roofing revealed that this roofing behaved similarly to the 900 mm span roofing. During experiments, identical local dimpling of crests as in Figure 6 occurred at approximately the same load of 890 N/f and an uplift pressure of 7.54 kPa. The corresponding FEA predictions were 905 N/f and 7.46 kPa. This is in agreement with previous research on corrugated roofing with different spans[8].

4.2 Trapezoidal Roofing Profile with wide Pans (Type A)

The FEA and experimental load-deflection curves for this roofing of 900 mm span are presented in Figure 7, and there is reasonable agreement between the two results.

As in the case of corrugated roofing, the uplift loading caused severe cross-sectional distortion of this roofing since the screwed ribs are separated by a wide pan (see Figure 8). Therefore this also led to a premature localised failure of the crests. At first the crests slightly dimpled, but not as severe as that in the case of corrugated roofing. This was followed by a membrane action of the region. The region around the fastener hole was yielding at this stage. During experiments this finally led to a localised pull-through failure as shown in Figure 9 at a load per fastener of 1365 N. The corresponding uplift pressure was 6.7 kPa. Experiments using air bag pressure loading gave a higher failure load per fastener of 1420 N and pressure of 7 kPa. Unlike the corrugated roofing, there was no reserve strength beyond this local pull-through failure. It is to be noted that there was no buckling or global yielding of the section elsewhere in the roofing.

The FEA showed that there were high membrane strains in the longitudinal direction. Since the high tensile steel used has limited ductility, a transverse fracture occurred at the fastener hole when the membrane stresses reached yielding. The transverse fracture thus let the fastener pull-through the roofing. Although the FEA confirmed the large membrane strains at these locations, it could not predict this pull-through failure load as it assumed perfect elastic-plastic material behaviour with infinite ductility. The FEA predicted a maximum load of 1470 N/f (uplift pressure 7.19 kPa), however, inspection of the stresses around the fastener hole indicate that the membrane stresses in the longitudinal direction reached yielding at about 1300 N/f. The longitudinal membrane strains appeared to have reached the failure strain value of 2% (from tensile tests) at about 1440 N/f. This means that the steel will fracture before the load of 1470 N/f. Based on this, the predicted pull-through failure load was in the range of 1340 and 1440 N/f, which agrees well with the experimental pull-through failure load. Further details of the behaviour of this roofing can be found elsewhere[11].

Experiments of a 600 mm span roofing were also conducted and they revealed that the behaviour was similar to that of the 900 mm span roofing, and that identical local pull-through failure (see Figure 9) occurred at approximately the same load of 1370 N/f (the corresponding uplift pressure = 10.5 kPa). This indicates that the load per fastener at the central support is the critical loading parameter for the cladding under wind uplift.

4.3 Trapezoidal Roofing Profile (Type B)

Figure 10 presents the FEA and experimental load-deflection curves for this roofing of 900 mm span, and the results are in reasonable agreement.

As in the case of other roof claddings, the uplift loading caused severe cross-sectional distortion of this roofing as shown in Figure 11 since the roofing was only fastened at alternate crests. Therefore this also led to a premature localised failure of the crests, but

the failure was of a mixed type between those of the other two roofing profiles. At first the local behaviour around the fastener holes was similar to the other trapezoidal roofing. There was slight dimpling, which was followed by a membrane action of the region. It was found that this similarity caused the Type A and B claddings to have similar fatigue behaviour under cyclic uplift wind loading[12]. The regions around the fastener holes began to yield soon after this stage. Following this the behaviour was somewhat like that of corrugated roofing, as the crests dimpled beyond the edges of the ribs as shown in Figure 12. Despite this, in most experiments, final failure occurred by a localised pull-through failure similar to that of the other trapezoidal roofing (see Figure 12) at a load of 1235 N/f. The corresponding uplift pressure was 6.24 kPa. As seen in Figure 10, the corresponding FEA values were 1240 N/f and 6.75 kPa.

In some experiments, the rib was completely flattened, but did not pull-through at the load at which this flattening occurred. Another crest at the central support developed further dimpling and eventually the roofing pulled through at this crest at a somewhat higher load. It is considered that this reserve strength cannot be guaranteed and thus the failure load was considered to be that at which the first crest failed locally. The reason for the pull-through failure can be attributed to the same reasons given for the Type A trapezoidal roofing. The FEA showed some large membrane strains in the region around the fastener hole, but not to the extent observed with the Type A trapezoidal roofing. This may explain the absence of pull-through failure during some experiments. It is to be noted that there was no buckling or global yielding of the section elsewhere in the roofing, indicating that the strength of the cladding was determined by the local failure at the crests.

Experiments on 600 and 1150 mm span roofing revealed that the local failure occurred at approximately the same load of 1190 and 1200 N/f, respectively, in comparison to the failure load of 1235 N/f for the 900 mm span. This indicates that the load per fastener at the central support is the critical loading parameter as observed with other roofing profiles.

It is noted that the corresponding uplift pressures were 10.6 and 5.23 kPa. The FEA of 600 mm span roofing also confirmed these results (1190 N/f and 9.75 kPa).

As observed in all the load-deflection curves shown in Figures 4, 7 and 10, the local failure load from the FEA and experiments agreed quite well, despite the fact that in some cases, the deflections did not agree well. This can be attributed to the fact that during experiments the deflections were not always measured at the crests which failed.

The fastener failure loads and the corresponding uplift pressures for all three roof claddings are summarised in Table 1.

5. Use of Small Scale Roofing Models

As seen during the experiments and confirmed by the FEA, the observed behaviour of all the roof claddings under wind uplift appears to be complicated, involving large cross-sectional distortion of the roofing from early stages of loading, followed by localised deformations and yielding of roofing around the fastener holes. Simple theories cannot be used to predict the largely nonlinear large deflection behaviour of these intermittently crest-fixed claddings. Eurocode[6] for the design of profiled steel roof claddings use the effective cross-section concept for the thick and softer claddings fastened at valleys. In this, the bending capacity of the cladding is calculated which includes moment-reaction interaction and web crippling effects. Alternatively, it is determined by testing. Similarly, the strength of connections is then determined either using testing or design formulae. The strength of the cladding system is governed by either the strength of the cladding or connections. Design tables for various spans are then produced, considering also the appropriate deflection limits. This procedure is not suitable for the crest-fixed cladding systems considered in this investigation. Eurocode provisions[6] assume that there is no cross-sectional distortion of claddings as observed in this investigation and that the

strength is governed by buckling considerations of the profile, and thus will not be able to predict the strength of the crest-fixed claddings.

As observed in this investigation, the static strengths of all the three roof cladding systems were determined by the load at which the local failure occurred at the central support fastener holes, i.e., by the pull-through or local dimpling strength of their screwed connections. During high wind events, the loading fluctuates randomly and causes cracking in the large stress concentration regions around the fastener holes[1]. This means that the fatigue strength of the cladding system is determined by the fatigue cracking near the fastener holes. Therefore it may be adequate to design these cladding systems based on the strength of their connections. The strength of the connections is dependent on the type of roofing profile, its thickness, strength and ductility of steel and also the type and size of fastener. Therefore the design of these cladding systems may have to be based on testing of two-span roofing assemblies as it is done currently. However, since it is clear that the static and fatigue strength of the full scale roof cladding system is governed by the strength of their screwed connections, a design method based on testing of small scale models of roofing around the central support fastener holes is recommended.

In this method, a small scale roofing of approximately 240 x 240 mm with the screw fastener at the middle as shown in Figure 13 was tested under tension loading of the fastener to determine the strength of the screwed connections of the roofing. Each dimension of roofing was only about 1.5 times the distance between fasteners. In the full scale roofing under wind uplift loading, the roofing around the fastener holes deflects upwards, but the roofing under the fastener head remains fixed. The small scale models were designed such that the reverse would occur. Thus roofing was fastened to a small rectangular wooden frame made of four 25 x 50 mm members to simulate appropriate boundary conditions. The transverse distance between the supports was equal to the distance between fasteners, i.e. pitch of the roofing for trapezoidal roofing - Type A and twice the pitch for corrugated and trapezoidal Type B roofing whereas the longitudinal

distance between the supports was 200 mm, being equal to 1.05 to 1.3 times the distance between fasteners. The central fastener was not actually fastened to the wooden frame, but was free to move vertically. It is noted that this small scale model simulated both longitudinal and transverse bending and membrane deformations of roofing which occurs in the full scale roof cladding.

The wind uplift loading on the small scale roofing models was simulated by applying a tension force in the fastener (see Figure 13). The specially made central fastener had the same fastener head, but was made to be about 200 mm long so that a load cell can be included within its length. Static wind uplift loading was simulated simply by tightening the long fastener. This means a static wind uplift loading test can be carried out to failure without the use of a testing machine. Recently this small scale model has been used satisfactorily to investigate the contrasting fatigue behaviour of corrugated and trapezoidal roofing profiles[12] and to study the pull-through strength of screwed connections[13]. These small scale tests are very simple and inexpensive to conduct. Further details of the validation of these small scale models are given elsewhere[12,13].

In this investigation the above-mentioned small scale roofing models produced the same local failures observed earlier with the full scale claddings (see Figures 6, 9 and 12) at approximately the same load per fastener levels. These failure loads based on a minimum of 4 tests in each case were on average 860 N/f for corrugated roofing, 1430 N/f for trapezoidal roofing with pans (Type A) and 1250 N/f for the other trapezoidal roofing (Type B). These values compare well with the corresponding experimental full scale values of 870, 1365 and 1235 N/f (900 mm span), and 890, 1370, 1190 N/f (600 mm span).

6. Design Method

The following design method is recommended for the crest-fixed steel roof cladding systems considered in this investigation. However, the same method can be used for other

similar cladding systems for which the strength of their screwed connections is the governing case. The proposed design method is similar to that recommended by the Eurocode[6] for connections in thin-walled sheeting and members. Since all the relevant loading and design codes will eventually be in the limit state format, ultimate strength values are used. In this method it is recommended that the characteristic pull-through/local dimpling strength of screwed connections in terms of load per fastener P_u is determined based on a statistical evaluation of experimental results using the small scale roofing models. Alternatively, a formula similar to that given by Equation (2) is derived in terms of the thickness t and the ultimate strength of steel σ_u for a given screw fastener. The fastener failure strength can then be used to determine the ultimate wind pressure.

$$P_u = k\, c\, t^2\, \sigma_u^{1/3} \qquad (2)$$

where c = Coefficient depends on the profile geometry and to be determined by small scale experiments and finite element analysis, and

k = 1 for static loading (non-cyclonic areas)

In this investigation a parametric study was carried out using FEA and small scale models for different thicknesses (0.35, 0.42 and 0.48 mm) of all three roofing profiles, and for different grade steels in order to verify the accuracy of Equation (2) for the No.14 screw fasteners (see Table 2). It is to be noted that the Australian roofing industry mainly uses a high tensile steel, the G550 steel, for which the ratio of yield to ultimate strength is very close to one (690 and 720 MPa) and the strain at failure is very small (2%). The observed pull-through failure mode (Figures 9 and 12) is attributable to the low failure strain of steel. Thus the above equation is recommended for roof claddings made of such high tensile steel. In such cases, the difference in using the yield stress as opposed to ultimate stress makes little difference, however, in this investigation the latter is used.

Based on Table 2 results the coefficient c can be taken as 0.54, 0.89, and 0.79 for the roofing profiles considered here (corrugated roofing, trapezoidal roofing - Type A and

Type B, respectively). For design purposes, the coefficient should be taken as 0.45, 0.74, 0.66 to allow for the characteristic strength based on 95% ~~percentile values~~ and 10% standard deviation.

As reflected by the exponents of t and σ_u in Equation (2), the strength was very much dependent on the thickness, and not so much on the strength of roofing material. Small scale model testing and FEA showed that when the screw shaft/hole diameter was changed (4.5, 5.5, 7.5 mm), the strength of crest-fixed connections changed only marginally for all three profiles. On the other hand increasing the screw head or washer diameter from 14.5 to 17.5 and 20 mm, there was significant increase in the strength of connections of trapezoidal roofing Type A, some increase for trapezoidal roofing Type B and none for corrugated roofing. For the strength of corrugated roofing to be improved, washers as big as the cyclone washers used currently in the cyclone prone areas have to be used. Thus it was decided not to include the screw diameter in Equation (2), which is then valid only for the common No.14 screw fasteners. However, for the other screw fasteners, only the coefficient c has to be changed based on test results. It is believed that the same coefficient c can be used for the other common No.12 screw fastener since the screw head diameter is almost the same as that of No.14 screw fastener. All these observations are in contrast to the European[6] and American[7] provisions, and it is believed to have arisen due to the crest-fixing instead of valley-fixing. It is noted that the above design formula was based on a limited number of analyses and experiments, and will be improved once more results become available from the ongoing investigation.

Once the pull-through/local dimpling strength of connections is determined either using small scale testing or the design formula (Equation (2)), ultimate design wind uplift pressure capacity of a multi-span crest-fixed roofing assembly can be determined using Equation (1). For the end spans of the assembly, Equation (1) can be used with the same coefficient α of 1.25. This value is recommended because it is conservative despite the scatter of α values in Table 1. Further experiments are needed to study the scatter of α

values which depends on the type of roofing and span. Similarly the ultimate design wind uplift pressure for the intermediate spans can be calculated using Equation (1) with an α value of 1.0. It is believed the same approach can be used for the deeper roofing profiles developed recently by the Australian roofing manufacturers.

For cyclonic areas, fatigue cracking failure[1,2] of crest-fixed roof claddings during cyclones should be eliminated by subjecting the cladding to a three level standard fatigue test consisting of 10,200 cycles[3,4]. At present this fatigue testing is conducted to determine the limiting load per fastener and uplift pressure. However, equation (2) can still be used with a smaller k value in the range of 0.5 to 0.8. It is noted that Eurocode[6] recommends a factor of 0.5 for repeated loading. Further investigations are needed before deciding on a conservative value of k that will suit most of the claddings. Alternatively, a suitable k value for each of the common roof claddings can be determined from fatigue tests.

It is noted that the other failure modes in the screwed connections such as the pull-out failure and screw fracture are not considered here since the pull-through failure occurs before them in the common roof cladding systems.

7. Conclusions

The following conclusions have been drawn from this investigation.

(1) The behaviour of crest-fixed steel roof claddings under wind uplift was very much dependent on the geometry of the profile. It may be possible to improve the static and fatigue performance of these roof claddings by minor changes to the geometry.

(2) Results from the finite element analysis and experiments agreed well for all three roof claddings used in this investigation.

(3) Because the thin claddings were only fastened intermittently at their crests, they underwent large cross-sectional distortion and localised deformations around the fastener holes when subjected to wind uplift. With all three claddings this mode of behaviour led to localised failure at the fastener holes by either pulling through or by dimpling of crests. There was no global roof cladding failure. This indicates that the load per fastener at the critical central support is the most important parameter. Therefore it is recommended that the design of these roof cladding systems can be based on the pull-through/local dimpling strength of their screwed connections. Suitable small scale models have been recommended for the determination of the strength of screwed connections.

(4) A simple design formula for the strength of screwed connections of the common roof claddings, and thus for the strength of the roof claddings under wind uplift in both cyclonic and non-cyclonic areas, has been recommended in a similar manner to that in Eurocode[6]. This will simplify the design of roof claddings under wind uplift without depending on extensive testing. However, since the formulae will be conservative, testing could be carried out to improve the design values. It is believed that these improvements to the design methods using small scale model testing and design formulae will lead to innovation and efficiency in the profiled roof sheeting industry.

8. Acknowledgements

The author wishes to thank Queensland University of Technology for the financial support, and Lysaght Building Industries and Buildex for donating the roofing materials. Thanks are also due to QUT students Messrs. G. Lambourne, P. Avery, S. Pribilovic, and P. Pearl who assisted the author with the laboratory experiments and finite element analysis, and Ms B. Whitaker from QUT's Computing Services for her help with the use of NASTRAN on the Convex computer.

9. References

1. Mahendran, M. Fatigue Behaviour of Corrugated Roofing under Cyclic Wind Loading, Civil Eng. Trans., I.E. Aust., 1990, Vol.32, No.4, pp.219-226.
2. Beck, V.R. and Stevens, L.K. Wind Loading Failures of Corrugated Roof Cladding, Civil Eng Trans, I.E. Aust., 1979, 21-1, pp. 45-56.
3. Standards Australia (SAA), AS1170.2 - SAA Loading Code, Part 2 : Wind Loads, 1989
4. Standards Australia (SAA), AS4040.3 Methods of Testing Sheet Roof and Wall Cladding, 1992
5. Standards Australia (SAA), AS1562 Design and Installation of Sheet Roof and Wall Cladding, Part 1: Metal, 1992
6. Eurocode 3 Design of Steel Structures, Part 1 - General Rules and Rules for Building, Annexe A - Cold-formed Thin-gauge members and Sheeting, Draft document CEN/TC250/SC3 - PT1A, Commission of the European Communities, August, 1992.
7. American Iron and Steel Institute, Specification for the Design of Cold-formed Steel Structural Members, 1986 Edition with 1989 Addendum, AISI, Washington, D.C., 1989
8. Mahendran, M. Static Behaviour of Corrugated Roofing under Simulated Wind Loading, Civil Eng. Trans., I.E. Aust., 1990, Vol.32, No.4, pp.211-218.
9. Lysaght Building Industries, LBI Reference Manual, 1987.
10. The Macneal-Schwendler Corporation, MSC/NASTRAN User's Manual, USA, 1991
11. Telue, Y. Behaviour of Trapezoidal Roof Cladding under Wind Uplift, Final Year Thesis, QUT, Brisbane, October 1992.
12. Mahendran, M. Contrasting Behaviour of Thin Steel Roof Claddings under Simulated Cyclonic Wind Loading, Proc. of the Eleventh Int. Specialty Conf. on Cold-formed Steel Structures, St.Louis, Missouri, USA, Oct. 1992, pp.245-256.
13. Mahendran, M. Pull-through Strength of Screwed Connections for Crest-fixed Profiled Steel Claddings, Proc. of the International workshop on Cold-formed Steel Structures, Sydney, Feb. 1993.

Table 1. Summary of Two-span Roof Cladding Results

Roofing Type	Width (mm)	Span (mm)	Fastener Failure Load(N/f		Uplift Pressure(kPa)		α in Eq. (1)	
			Expt	FEA	Expt	FEA	Expt	FEA
Corrugated	152	600	890	905	7.54	7.46	1.29	1.31
		900	870	815	5.27	5.18	1.21	1.15
Trapezoidal	190	600	1370	-	10.5	-	1.15	-
Type A		900	1365	1390	6.70	6.80	1.19	1.20
Trapezoidal	174	600	1190	1190	10.6	9.75	1.08	1.17
Type B		900	1235	1240	6.24	6.75	1.26	1.17
		1150	1200	-	5.23	-	1.15	-

Note: Width (mm) is the distance between fasteners

Table 2. Accuracy of Equation (2)

Roofing Type	t (mm)	σ_u (MPa)	Fastener Failure Load (N/f)			c in Eq.2 (Ave.)
			Experiment		FEA	
			Two-span	Small scale	Two-span	
Corrugated	0.42	720	880	860	860	0.55
	0.42	575	-	-	785	0.54
	0.42	315	-	-	660	0.55
	0.35	720	-	560	580	0.52
	0.48	720	-	1080	1095	0.53
Trapezoidal Type A	0.42	720	1365	1430	1390	0.88
	0.42	575	-	-	1330	0.91
	0.42	315	-	-	1040	0.87
	0.35	720	-	970	1000	0.89
	0.48	720	-	1800	1935	0.90
Trapezoidal Type B	0.42	720	1210	1250	1215	0.78
	0.42	575	-	-	1150	0.78
	0.42	315	-	-	925	0.77
	0.48	720	-	1700	1655	0.81

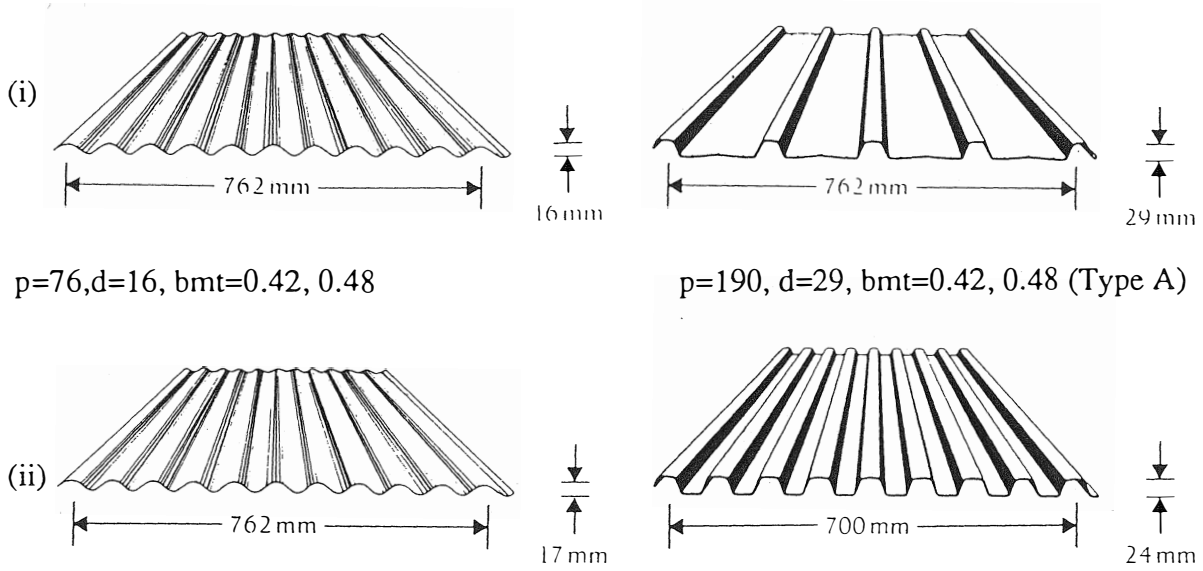

(a) Corrugated Roofing Profiles (b) Trapezoidal Roofing Profiles

Note : bmt = Base Metal Thickness (mm), p = Pitch (mm), d = Depth (mm)

Roofing material yield strength (minimum) = 550 MPa, except for (a) (ii)300 MPa

Figure 1. Profiled Steel Roof Claddings in Australia

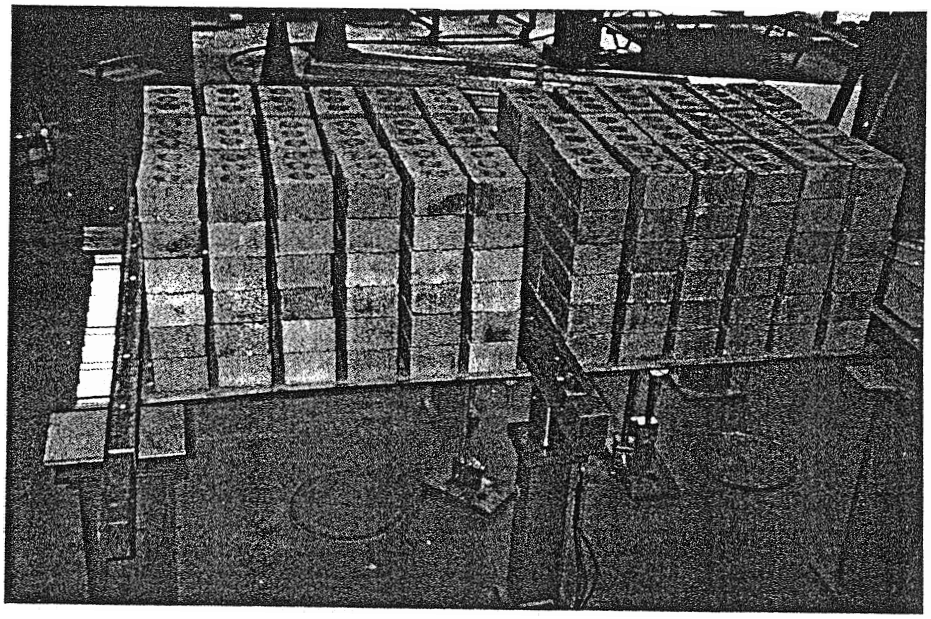

Figure 2. Test Set-up

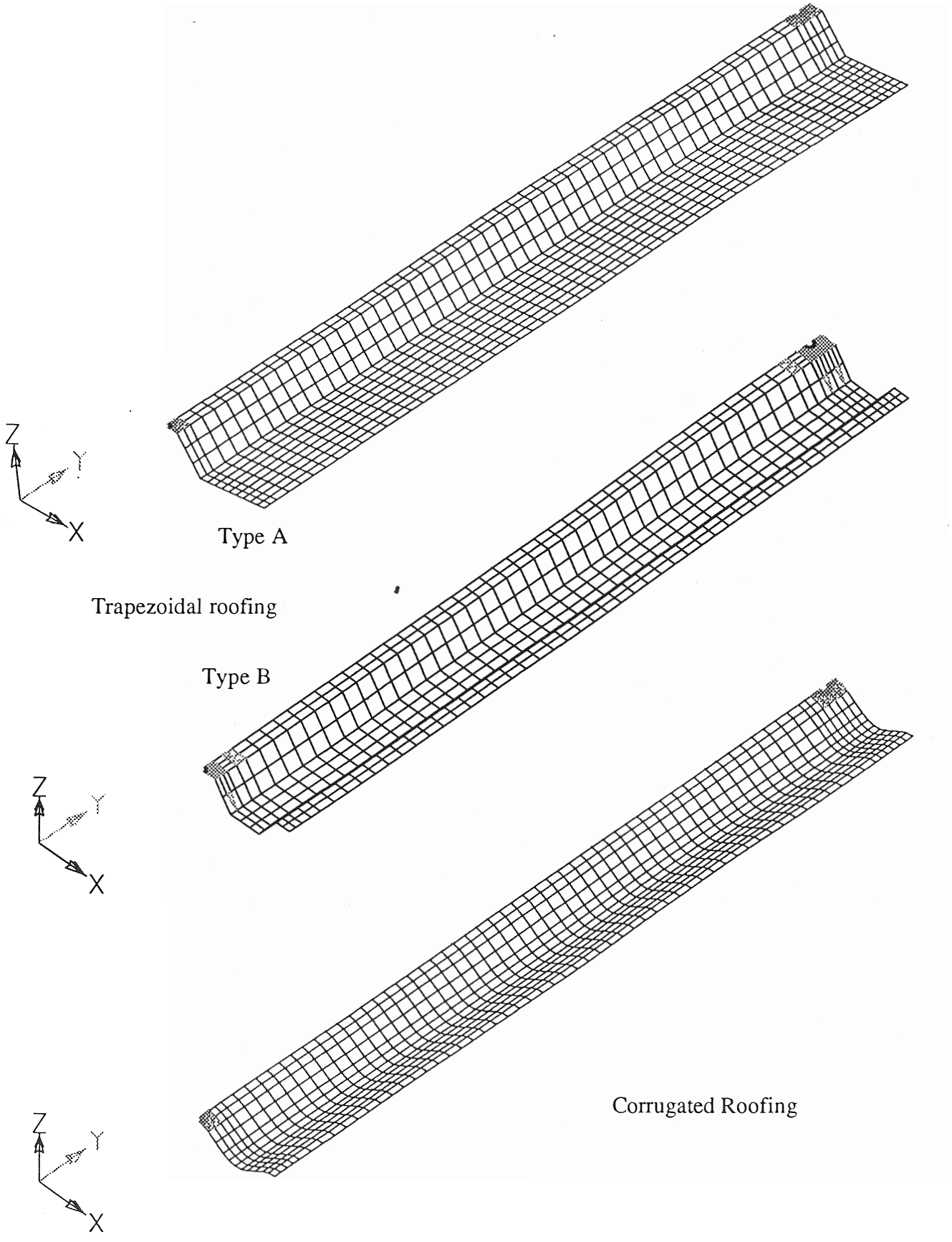

Figure 3. Finite Element Meshes of Roof Claddings

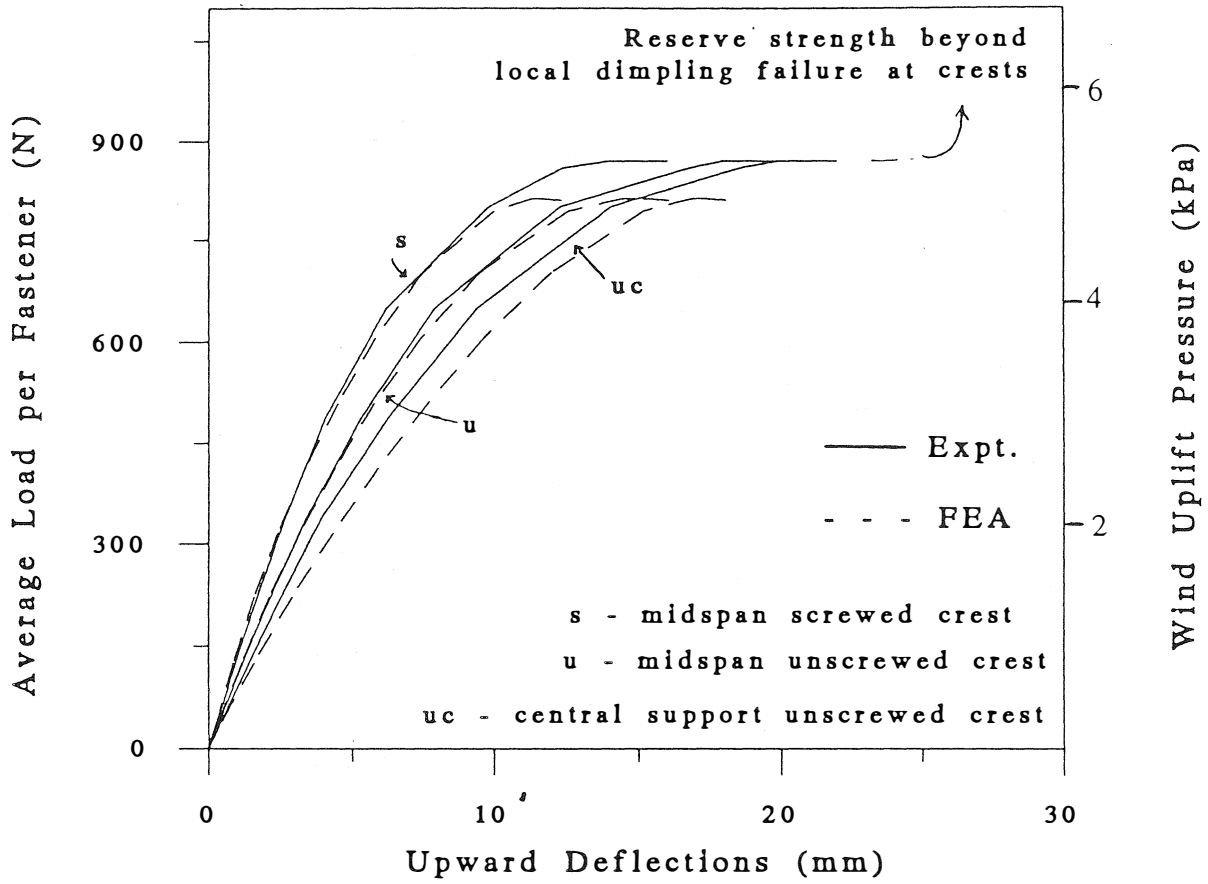

Figure 4. Load-deflection Curves for Corrugated Roofing

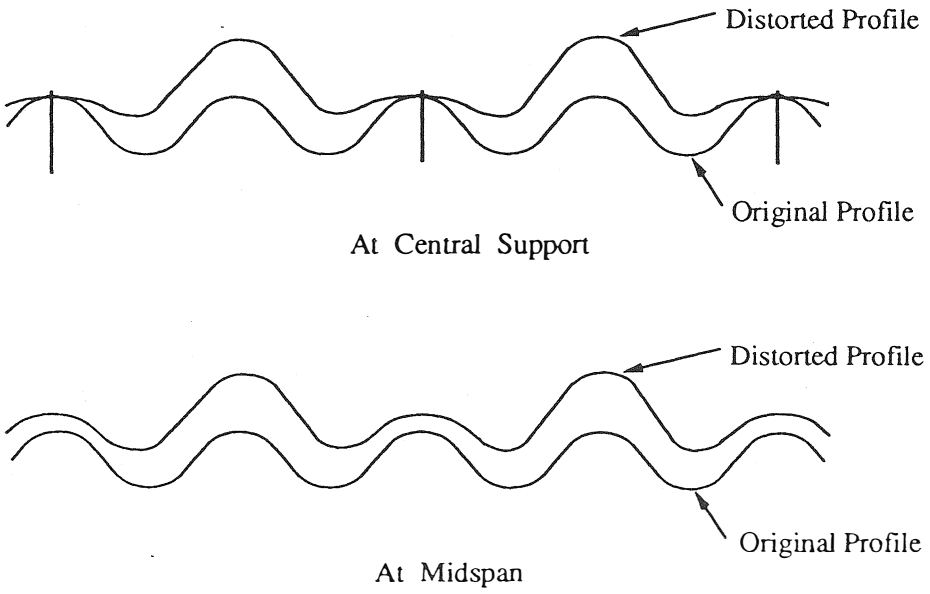

Figure 5. Cross-sectional Distortion of Corrugated Roofing

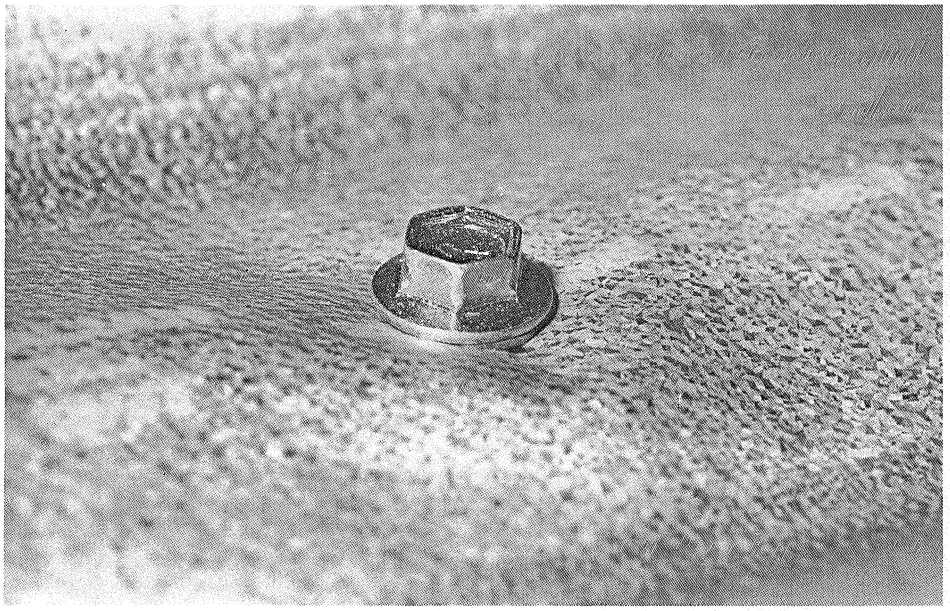

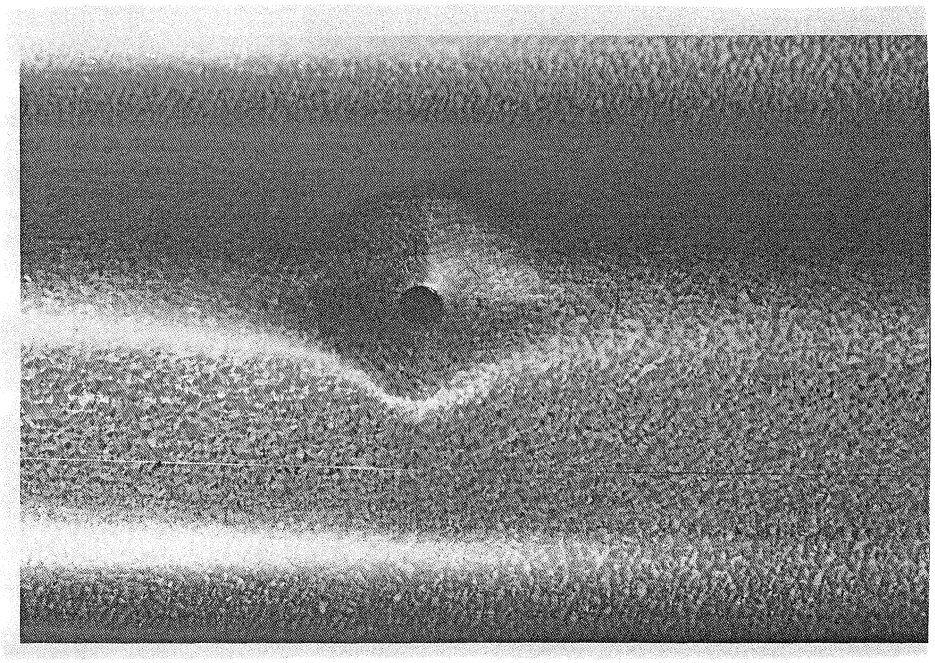

Figure 6. Local Dimpling Failure at Crests

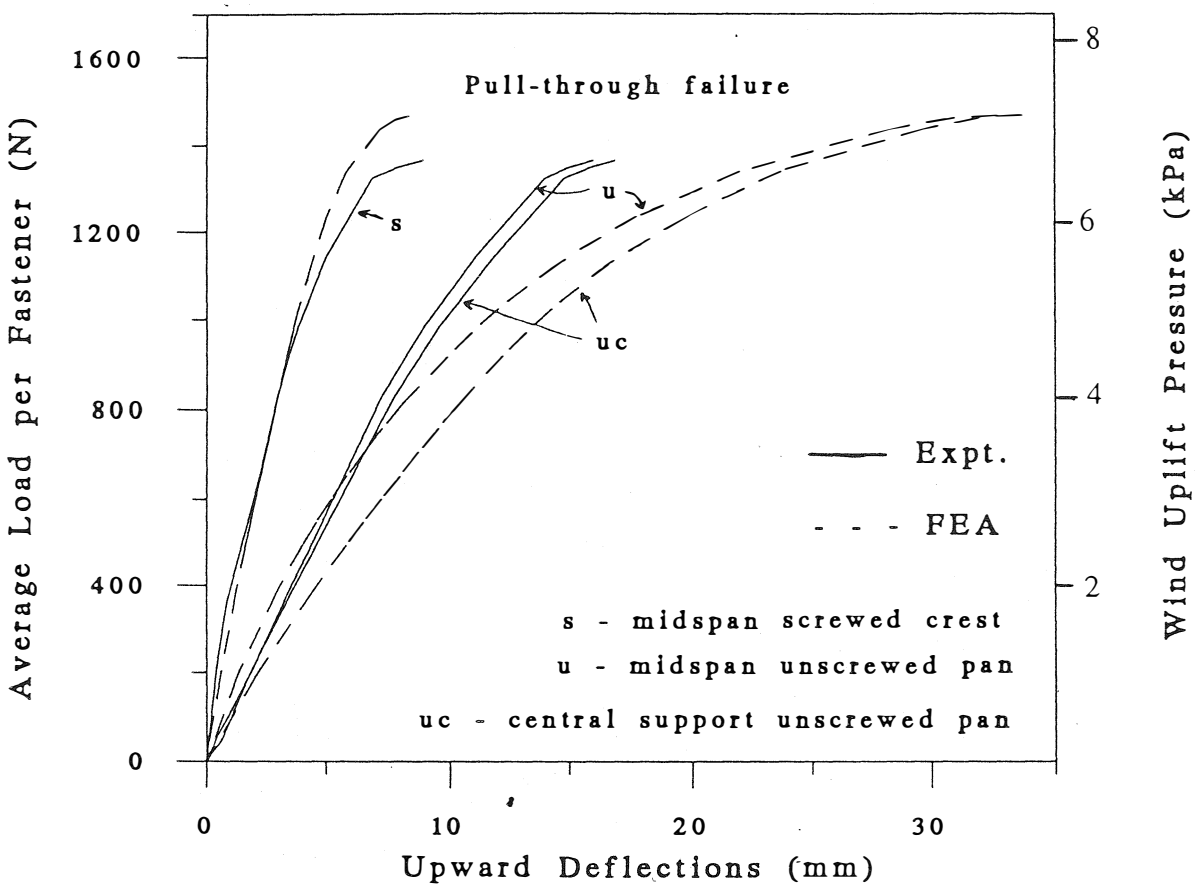

Figure 7. Load-deflection Curves for Trapezoidal Roofing - Type A

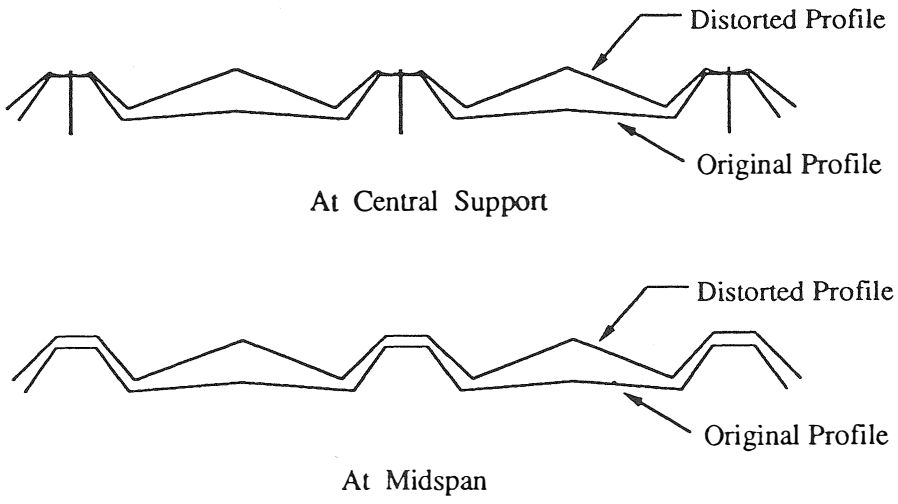

Figure 8. Cross-sectional Distortion of Trapezoidal Roofing - Type A

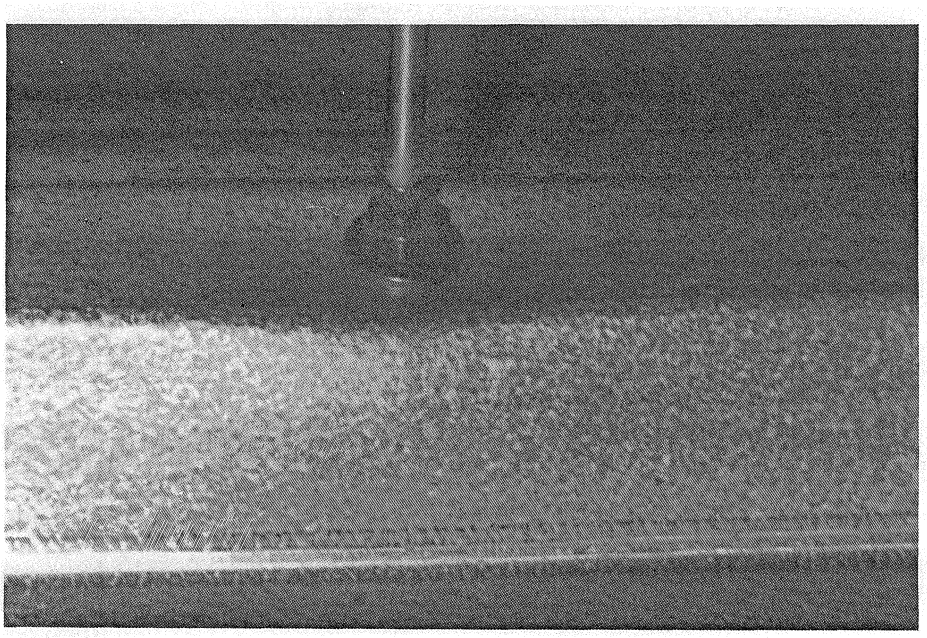

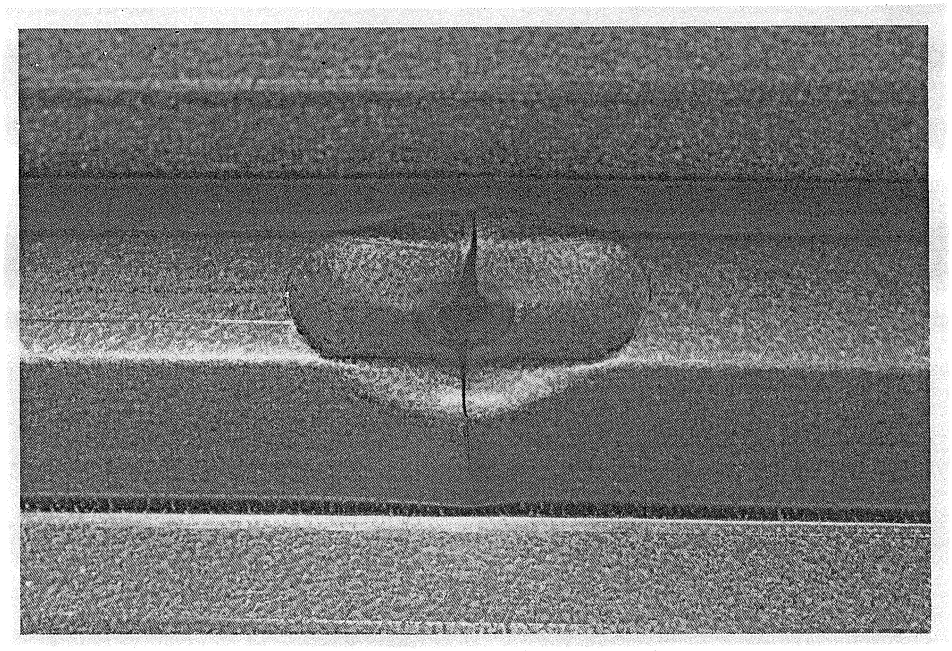

Figure 9. Local Pull-through Failure at Crests

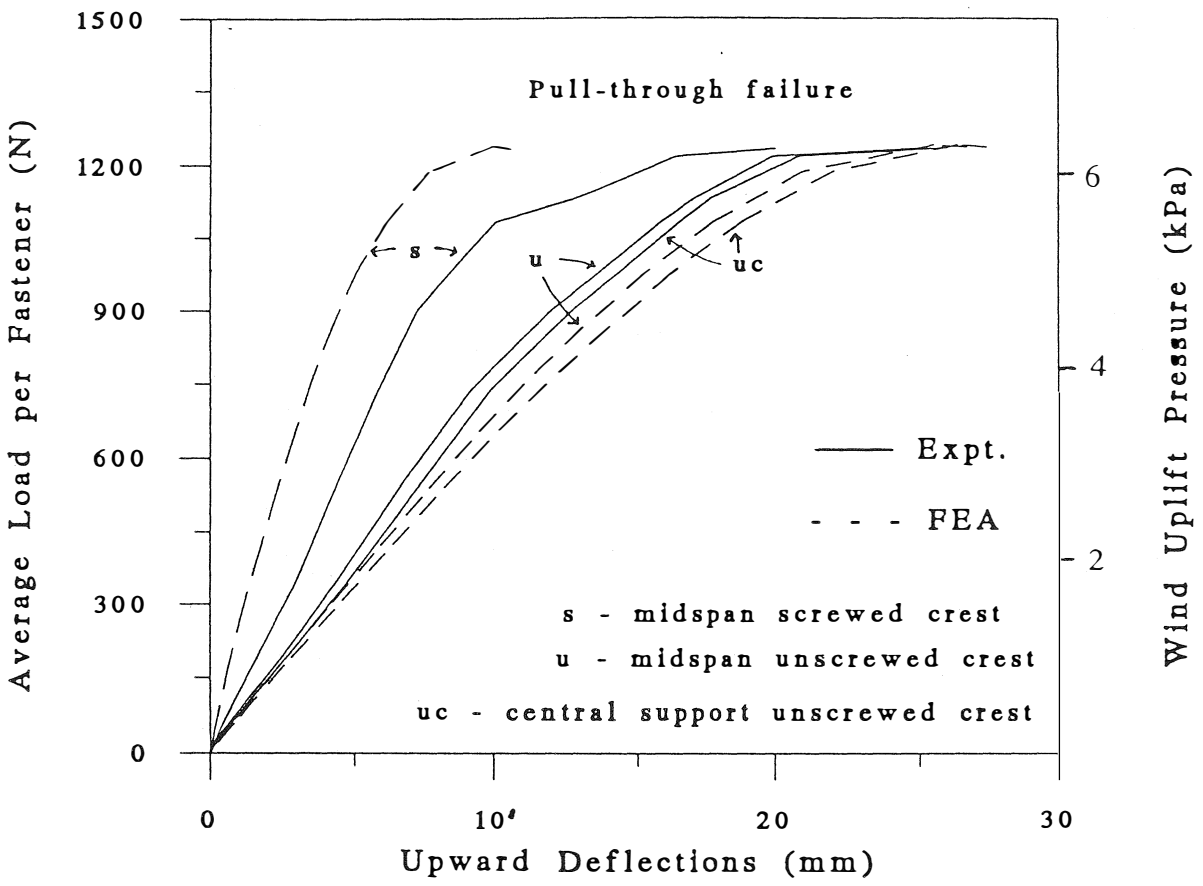

Figure 10. Load-deflection Curves for Trapezoidal Roofing - Type B

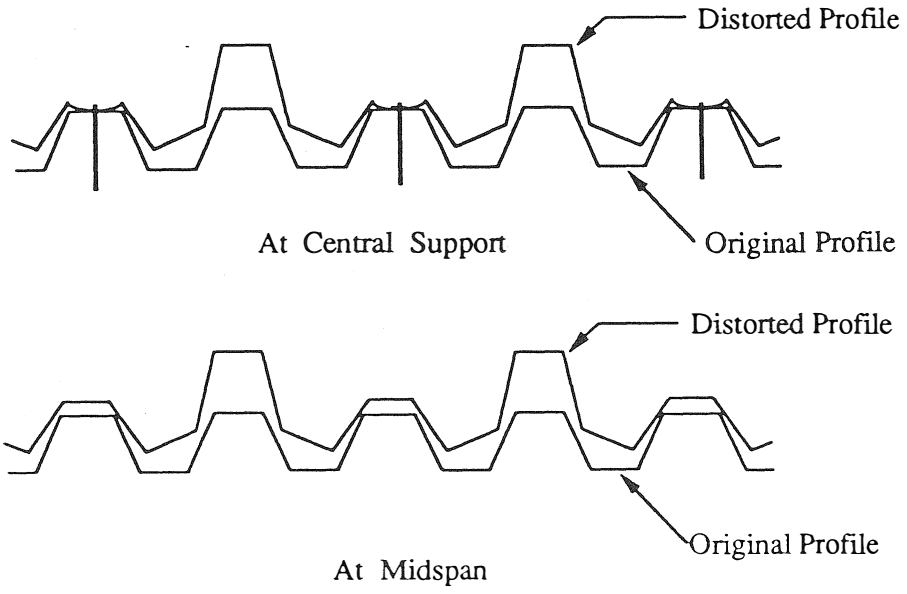

Figure 11. Cross-sectional Distortion of Trapezoidal Roofing - Type B

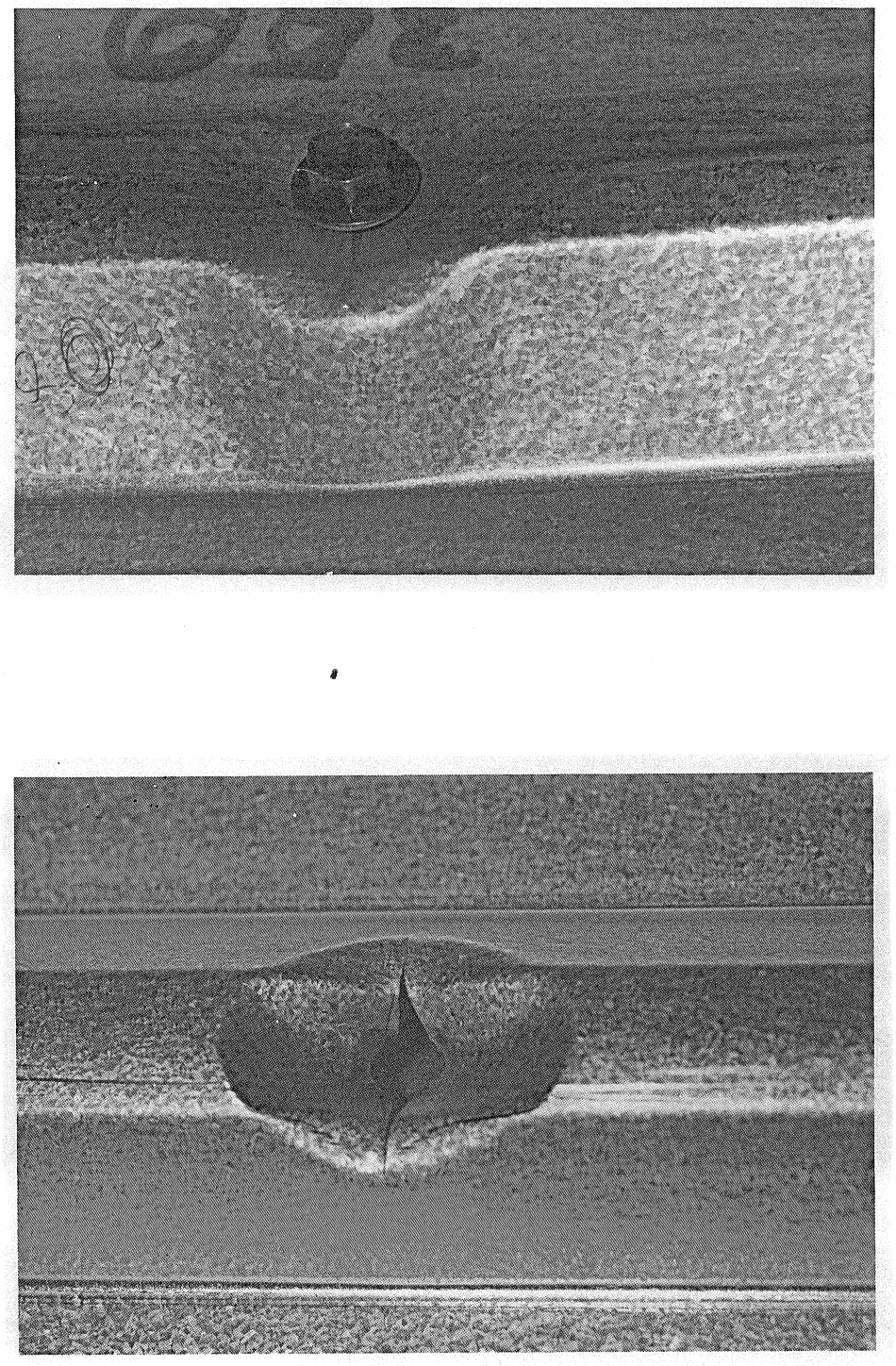

Figure 12. Local Dimpling/Pull-through Failure at Crest

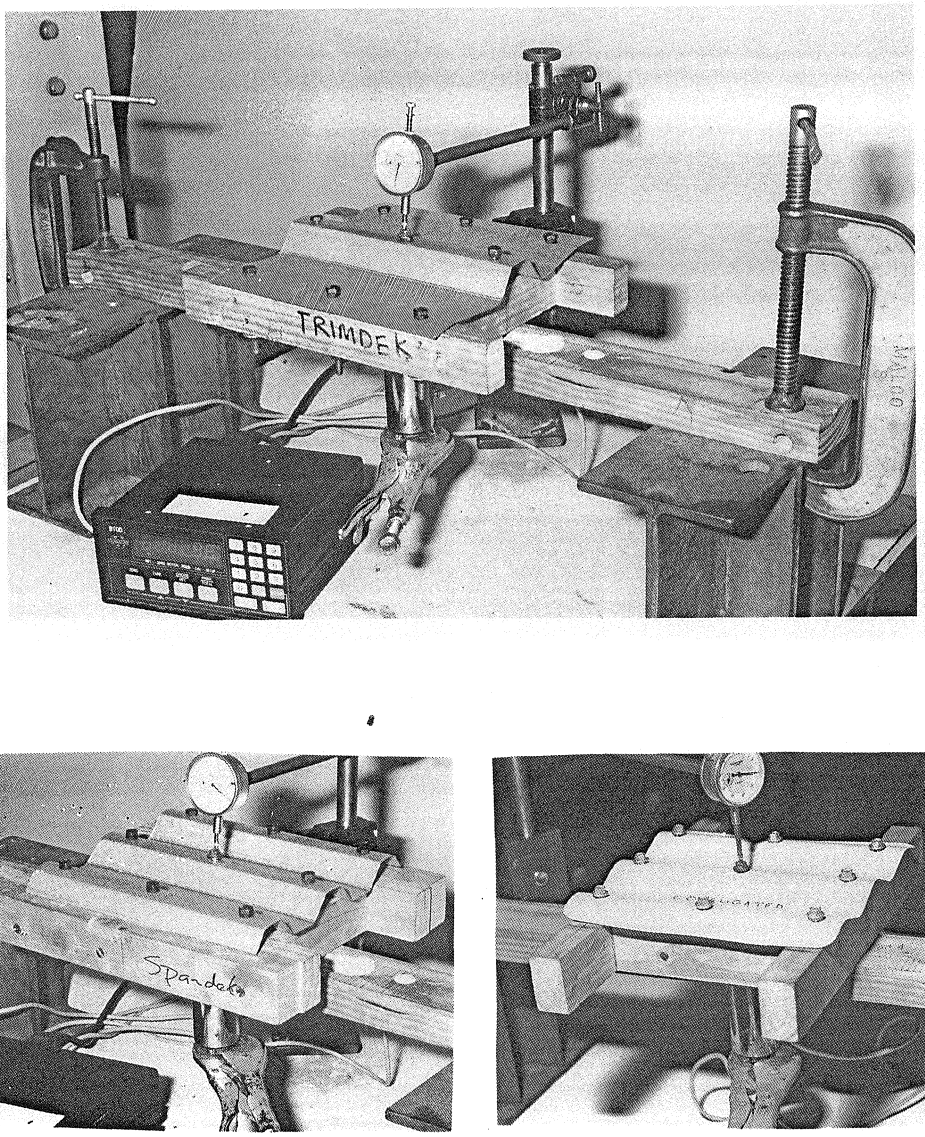

Figure 13. Small Scale Models Simulating Wind Uplift on Roof Claddings